Available online at www.sciencedirect.com
SCIENCE DIRECT®
Journal of Sound and Vibration 270 (2004) 1013–1032
JOURNAL OF SOUND AND VIBRATION
www.elsevier.com/locate/jsvi

Experimental and theoretical study on crack detection in pipes filled with fluid

S.M. Murigendrappa, S.K. Maiti*, H.R. Srirangarajan

Department of Mechanical Engineering, Indian Institute of Technology Bombay, Mumbai-400 076, India

Received 25 July 2002; accepted 12 February 2003

Abstract

The possibility of representing a crack with straight front, normal to the axis, and part through-the-thickness in a straight pipe containing fluid under pressure, by a spring for simulating its transverse free vibration has been examined experimentally. The fluid considered is water. Two different materials; aluminium and mild steel have been examined. Crack size to pipe thickness ratio ranging from 0.19 to 0.64 is considered. Within the fluid (gauge) pressure range of 0–0.981 MPa examined, the stiffnesses obtained by deflection- and natural frequency-based methods show good agreement. This indicates that the representation of a crack by the rotational spring is reasonably accurate. The natural frequency-based method can also be used to detect the location of an unknown crack in the pipeline. This has also been examined. The maximum error in prediction is 2.6% for all the cases considered. Data presented on variation of rotational spring stiffness vs. ratio of crack size to thickness can be very useful in crack size detection in pipelines knowing the spring stiffness. The error in the crack size prediction using these plots lies in the range −16.44% to 10.30% for aluminium and −5.83% to 12.04% for mild steel.

1. Introduction

Non-destructive testing (NDT) methods are often employed for detection of cracks in machine and structural components. Although a number of accurate, effective and reliable NDT methods based on X-ray, ultrasonic, magnetism, etc., are available, their adoption becomes uneconomical for long beams and pipelines which are widely met in power plants, chemical plants and offshore oil installations, etc. In order to detect a crack by any of these methods, the whole component requires scanning. This makes the process tedious and time consuming, and the cost involved may make the application prohibitive. This has motivated development of alternative methods.

*Corresponding author. Tel.: +91-022-576-7526; fax: +91-022-572-3480.
E-mail address: skmaiti@me.iitb.ernet.in (S.K. Maiti).

0022-460X/03/$ - see front matter © 2003 Elsevier Science Ltd. All rights reserved.
doi:10.1016/S0022-460X(03)00198-6

Vibration-based method of crack detection is considered to be a potential candidate and a lot of efforts [1–21] are now directed in this direction. The method can help to determine the location and size of a crack from the signatures collected from a single point on the component. Chaudhari and Maiti [16] have shown the effectiveness of the method based on frequency measurements for beam with rectangular, I-section and circular hollow sections. Pipes are of special concern here. Most often they are not empty and can contain materials, e.g., a fluid. Possibility of detection of a crack based on the vibration method in such components, when the fluid is static and under pressure has not been examined. This has provided the main motivation for the present study.

The method of crack detection requires a convenient way of modelling free vibration of the beam with a crack. Some investigators have represented the crack by reducing the section modulus around the crack locally. Others have represented it by a rotational spring, which adds an extra rotational flexibility or acts as an energy sink. For rectangular beams with through-the-thickness crack the rotational spring stiffness can be calculated from the knowledge of a relationship between stress intensity factor (SIF) and crack size. Readymade relations are also available [22]. Such a relationship is not available for a round pipe with a crack with straight front and part through-the-thickness. The rotational spring stiffness can be helpful in solving the forward problem of determination of frequencies knowing the crack details and the inverse problem of determination of location and crack size knowing, for example, the natural frequencies. Therefore determination of the rotational spring stiffness can serve useful purposes. The stiffness can be determined experimentally through measurement of deflections. It can also be obtained through frequency measurements in conjunction with inverse vibration analysis. A comparison of the results based on the two approaches and a comparison of predicted crack locations with the exact positions have been done. This study helps to comment on the possibility of adoption of the spring-based representation of a crack and its detection through measurement of natural frequency in such pipes.

2. Formulation for free vibration of pressurized pipe with crack

For a straight long pipe without any crack filled with an incompressible fluid, neglecting effects of shear deformation, rotational inertia and damping, the mode-shape equation is given [23] by

$$w'''' + \frac{A_i p L^2}{EI} w'' - \frac{\omega^2 L^4 (A_p \rho_p + A_i \rho_f)}{EI} w = 0, \tag{1}$$

where ω is the natural frequency, w is the transverse displacement, L is the pipe length, E is Young's modulus of elasticity, I is the second moment of area of cross-section, ρ_p is the density of material of pipe, ρ_f is the density of fluid, A_i and A_p are cross-sectional area of fluid cylinder and pipe, respectively, p is fluid pressure and prime indicates differentiation with respect to x. The general solution of Eq. (1) involves four arbitrary constants, which are determined from boundary conditions.

A simply supported pipe with a crack with straight front and part through-the-thickness, i.e., a non-leaking crack, is split into two segments, which can be connected by a rotational spring at the crack location (Fig. 1). The governing equation of motion for each segment is of the type of Eq. (1). Thereby, the mode-shape will involve eight arbitrary constants $C_1, C_2, C_3, \ldots C_8$. There

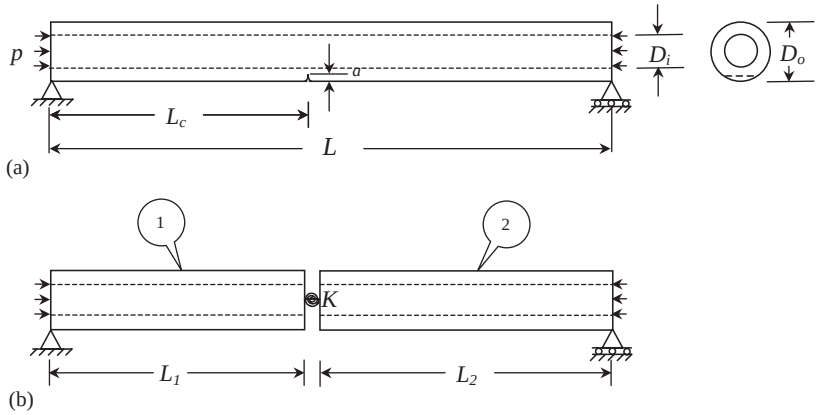

Fig. 1. (a) Schematic diagram of simply supported pipe with crack. (b) Representation by roational spring.

will be four boundary conditions and four compatibility equations at the crack location, $\beta(L_c/L)$, where L_c is the length from left end to crack. The last four are given below:

$$w_1(\beta) = w_2(\beta), \quad w_1'(\beta) + EI\frac{w_1''(\beta)}{K} = w_2'(\beta), \quad w_1''(\beta) = w_2''(\beta) \text{ and } w_1'''(\beta) = w_2'''(\beta), \tag{2}$$

where w_1 and w_2 stands for displacement for the two pipe segments, and K is the rotational spring stiffness. The above conditions are based on the assumption that there is a continuity of deflection, moment, and shear force, and a jump in slope. With eight conditions it is possible to obtain the characteristic equation for the cracked pipe in terms of a matrix of order 8. By giving the spring stiffness K as input it is also possible to solve for the natural frequencies from the characteristic equation [10].

Through the transfer matrix method [13] the characteristic equation which involves a matrix of smaller size is obtained. The state vectors associated with the right end $\{\mathbf{w}\}_{Right}$ of the pipe can be written in terms of those of the left end $\{\mathbf{w}\}_{Left}$ as follows:

$$\{\mathbf{w}\}_{Right} = [\mathbf{S}]_2[\mathbf{S}]_3[\mathbf{S}]_1\{\mathbf{w}\}_{Left}, \tag{3}$$

where $[\mathbf{S}]_1, [\mathbf{S}]_2$ and $[\mathbf{S}]_3$ are the transfer matrices of pipe segments and at the crack vicinity [13], respectively, and are given below:

$$[\mathbf{S}]_i = \begin{bmatrix} S_{11}^i & S_{12}^i & S_{13}^i & S_{14}^i \\ S_{21}^i & S_{22}^i & S_{23}^i & S_{24}^i \\ S_{31}^i & S_{32}^i & S_{33}^i & S_{34}^i \\ S_{41}^i & S_{42}^i & S_{43}^i & S_{44}^i \end{bmatrix}, \quad i = 1, 2, \tag{4}$$

$$[\mathbf{S}]_3 = \begin{bmatrix} 1 & 0 & 0 & 0 \\ 0 & 1 & \frac{1}{K} & 0 \\ 0 & 0 & 1 & 0 \\ 0 & 0 & 0 & 1 \end{bmatrix}, \tag{5}$$

where

$$S_{11}^i = \frac{\phi_2^2 \cosh \Omega_i + \phi_1^2 \cos \Theta_i}{\lambda_1}, \quad S_{12}^i = \frac{\phi_2^3 \sinh \Omega_i}{\varphi_1} + \frac{\phi_1^2 \sin \Theta_i}{\varphi_2}, \quad S_{13}^i = \frac{\cosh \Omega_i - \cos \Theta_i}{EI\lambda_1},$$

$$S_{14}^i = \frac{\sinh \Omega_i}{EI\varphi_1} - \frac{\sin \Theta_i}{EI\varphi_2}, \quad S_{21}^i = \frac{\phi_1\phi_2^2 \sinh \Omega_i - \phi_1^2\phi_2 \sin \Theta_i}{\lambda_1}, \quad S_{22}^i = \frac{\phi_2^2 \cosh \Omega_i + \phi_1^2 \cos \Theta_i}{\lambda_1},$$

$$S_{23}^i = \frac{\phi_1 \sinh \Omega_i + \phi_2 \sin \Theta_i}{EI\lambda_1}, \quad S_{24}^i = \frac{\cosh \Omega_i - \cos \Theta_i}{EI\lambda_1}, \quad S_{31}^i = \frac{EI\lambda_2(\cosh \Omega_i - \cos \Theta_i)}{\lambda_1},$$

$$S_{32}^i = EI\lambda_2\left(\frac{\sinh \Omega_i}{\varphi_1} - \frac{\sin \Theta_i}{\varphi_2}\right), \qquad S_{33}^i = \frac{\phi_1^2 \cosh \Omega_i + \phi_2^2 \cos \Theta_i}{\lambda_1},$$

$$S_{34}^i = \frac{\phi_1^2 \sinh \Omega_i}{\varphi_1} + \frac{\phi_2^2 \sin \Theta_i}{\varphi_2}, \qquad S_{41}^i = \frac{EI\lambda_2(\phi_1 \sinh \Omega_i + \phi_2 \sin \Theta_i)}{\lambda_1},$$

$$S_{42}^i = EI\lambda_2\left(\frac{\phi_1 \cosh \Omega_i}{\varphi_1} - \frac{\phi_2 \cos \Theta_i}{\varphi_2}\right), \qquad S_{43}^i = \frac{\phi_1^3 \sinh \Omega_i - \phi_2^3 \sin \Theta_i}{\lambda_1},$$

$$S_{44}^i = \frac{\phi_1^3 \cosh \Omega_i}{\varphi_1} + \frac{\phi_2^3 \cos \Theta_i}{\varphi_2},$$

$$\lambda_1 = \phi_1^2 + \phi_2^2, \qquad \lambda_2 = \phi_1^2\phi_2^2, \qquad \varphi_1 = \phi_1^3 + \phi_2^2\phi_1, \qquad \phi_2 = \phi_2^3 + \phi_1^2\phi_2,$$

$$\phi_{1,2} = \frac{\left[\mp A_i p/EI + \left\{\left(A_i p/EI\right)^2 + 4\omega^2(A_i\rho_f + A_p\rho_p)/EI\right\}^{1/2}\right]^{1/2}}{2},$$

$$\Omega_1 = \phi_1 L_1 \quad \text{and} \quad \Theta_1 = \phi_2 L_1 \text{ for } i = 1,$$
$$\Omega_2 = \phi_1 L_2 \quad \text{and} \quad \Theta_2 = \phi_2 L_2 \text{ for } i = 2,$$
$$L_1, L_2 = \text{length of segments 1 and 2.}$$

The following characteristic equation is obtained after inserting the boundary conditions:

$$\det\begin{bmatrix} A_{11} + \dfrac{B_{11}}{K} & A_{12} + \dfrac{B_{12}}{K} \\ A_{21} + \dfrac{B_{21}}{K} & A_{22} + \dfrac{B_{22}}{K} \end{bmatrix} = 0. \tag{6}$$

Alternatively, Eq. (6) can be written in the following form and it can be used to solve the inverse problem:

$$(A_{12}A_{21} - A_{11}A_{22})K - (A_{11}B_{22} + A_{22}B_{11} - A_{12}B_{21} - A_{21}B_{12}) = 0, \tag{7}$$

where

$$A_{11} = r_3r_1 + s_3s_1 + t_3t_1 + u_3u_1, \qquad A_{12} = r_3r_2 + s_3s_2 + t_3t_2 + u_3u_2,$$

$$A_{21} = r_4r_1 + s_4s_1 + t_4t_1 + u_4u_1, \qquad A_{22} = r_4r_2 + s_4s_2 + t_4t_2 + u_4u_2,$$

$$B_{11} = s_3 t_1, \qquad B_{12} = s_3 t_2, \qquad B_{21} = s_4 t_1, \qquad B_{22} = s_4 t_2,$$

$$r_1 = S^1_{12}, \qquad r_2 = S^1_{14}, \qquad r_3 = S^2_{22}, \qquad r_4 = S^2_{31},$$

$$s_1 = S^1_{11}, \qquad s_2 = S^1_{13}, \qquad s_3 = \left(\frac{\phi_2^2 \sinh \Omega_2}{\varphi_1} - \frac{\phi_1^2 \sin \Theta_2}{\varphi_2}\right), \qquad s_4 = S^2_{32},$$

$$t_1 = EI\lambda_2\left(\frac{\sinh \Omega_1}{\varphi_1} - \frac{\sin \Theta_1}{\varphi_2}\right), \qquad t_2 = S^1_{34}, \qquad t_3 = S^2_{24}, \qquad t_4 = S^2_{33},$$

$$u_1 = S^1_{42}, \qquad u_2 = \frac{\phi_1^3 \cos h\Omega_1}{\varphi_1} + \frac{\phi_2^3 \cos \Theta_1}{\varphi_2}, \qquad u_3 = \frac{\sinh \Omega_2}{EI\varphi_1} - \frac{\sin \Theta_2}{EI\varphi_2}, \qquad u_4 = S^2_{44}.$$

3. Rotational spring stiffness

The change in strain energy of a pipe with and without a crack under the action of a constant transverse load is equal to the energy released due to the crack. That is,

$$\Delta U = \int_{A_c} \frac{K_I^2}{2E} \mathrm{d}A = U_c - U_{nc}, \tag{8}$$

where K_I is the SIF for first mode crack, U_c and U_{nc} are strain energy of the crack and uncracked pipe and A_c is area of crack. When the rotational spring is used to represent the crack, this energy released gets stored in the spring. This is also given by

$$\Delta U = \frac{M^2_{empty\ pipe}}{2K}, \tag{9}$$

where $M_{empty\ pipe} = FL_1L_2/L + W_P LL_1/2 - W_P L_1^2/2$ is bending moment at the crack section due to loading F and self-weight W_P and K is the rotational spring stiffness. The difference ΔU can be calculated by applying a load F on the pipe and measuring the deflections in the two cases. That is,

$$\Delta U = U_c - U_{nc} = \frac{F(\delta_c - \delta_{nc})}{2}, \tag{10}$$

when the pipe is empty and δ_{nc} and δ_c are the corresponding deflections along the load line. Therefore,

$$K = \frac{M^2_{empty\ pipe}}{F(\delta_c - \delta_{nc})}. \tag{11}$$

For the case of a pipe with a fluid under pressure, considering the weight of fluid and pipe and its contributions to deflections, it is again possible to write

$$\Delta U = \frac{M^2_{fluid\ filled\ pipe}}{2K}, \tag{12}$$

where $M_{fluid\ filled\ pipe} = FL_1L_2/L + W_{FP}LL_1/2 - W_{FP}L_1^2/2 - A_i p\delta_{nc}$, W_{FP} is the total weight of the fluid and pipe material per unit length.

4. Experimental determination of rotational spring stiffness K

Experiments were considered to determine the rotational spring stiffness K using two techniques, which are based on deflection and vibration. Specimens were made out of aluminium and mild steel pipes. Tests were conducted with empty and water-filled pipes. Both pressurized

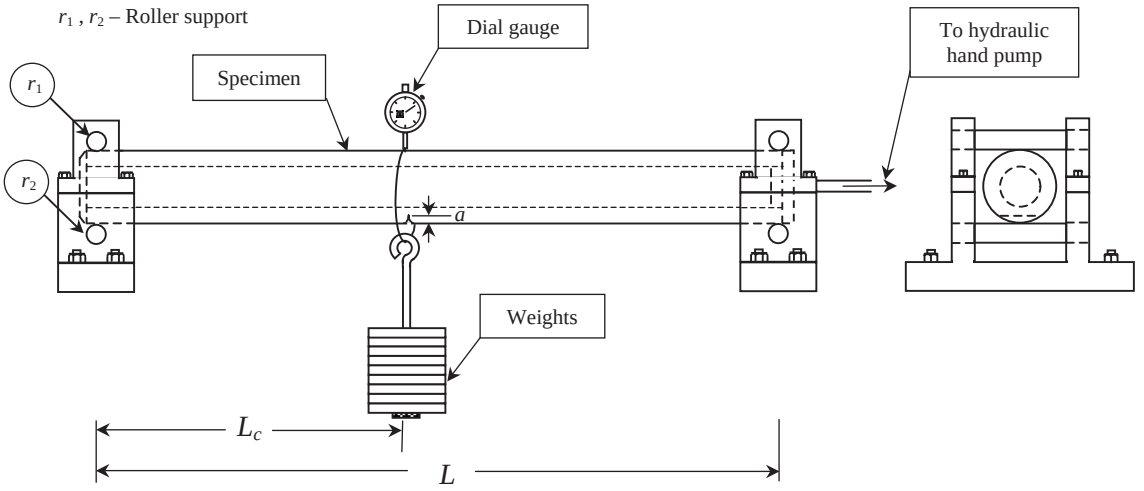

Fig. 2. Schematic of experimental setup for measurement of static deflection.

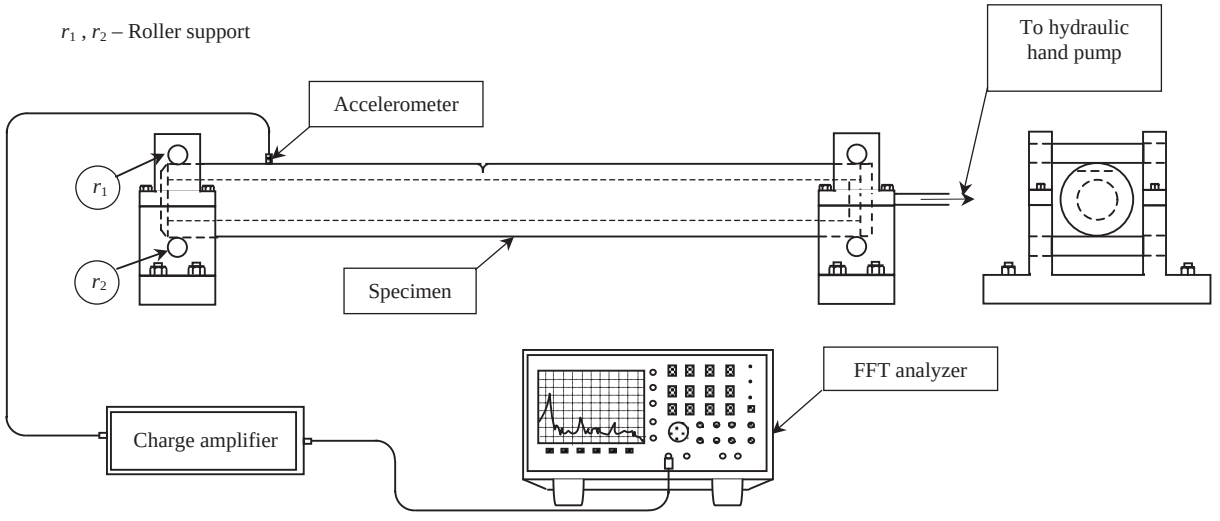

Fig. 3. Schematic of experimental setup for frequency measurement.

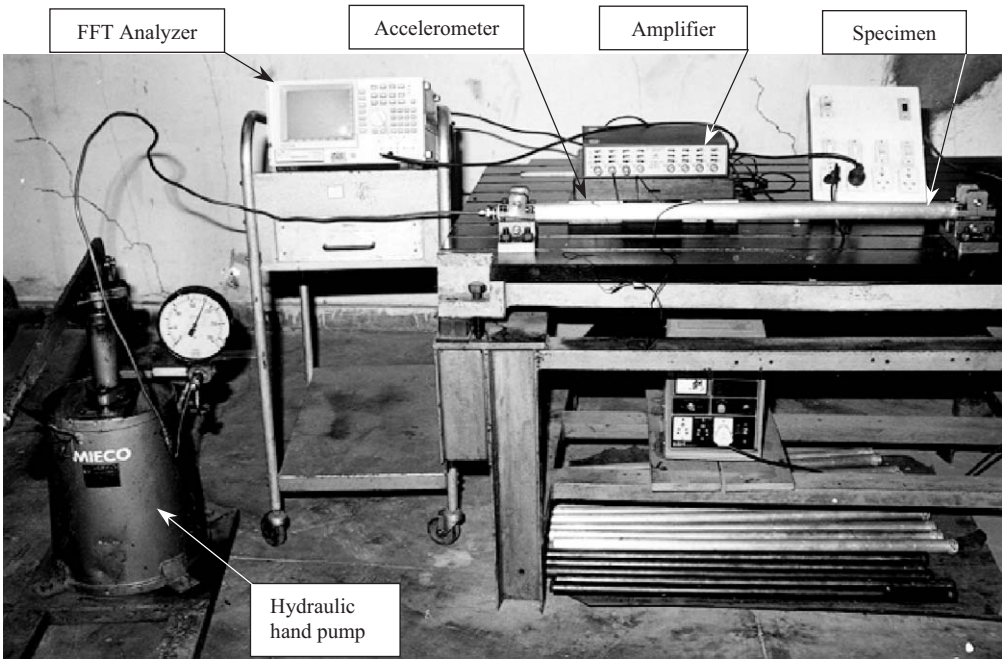

Fig. 4. Photograph of experimental setup for frequency measurement.

Table 1
Various dimensional combinations of specimens

Parameter	Case											
	1	2	3	4	5	6	7	8	9	10	11	12
Aluminium: $L = 0.7$ m, $D_o = 0.033$ m, $D_i = 0.02$ m, $F = 147.15$ N												
a/t	0.19043	0.19043	0.19043	0.25385	0.25385	0.25385	0.38077	0.38077	0.38077	0.6346	0.6346	0.6346
β	0.50000	0.47290	0.44290	0.50000	0.47290	0.44290	0.50000	0.47290	0.44290	0.5000	0.4729	0.4429
Mild steel: $L = 0.74$ m, $D_o = 0.032$ m, $D_i = 0.0195$ m, $F = 147.15$ N												
a/t	0.2032	0.2032	0.3040	0.3040	0.4064	0.4064	0.5080	0.5080				
β	0.2162	0.1892	0.2162	0.1892	0.3514	0.3243	0.3514	0.3243				

and no pressure conditions were examined. Two water pressures (gauge) were considered: 0.4905 and 0.981 MPa. All tests were carried out with simply supported end conditions. Aluminium pipe details are: length $L = 0.89$ m, external diameter $D_o = 0.033$ m and internal diameter $D_i = 0.02$ m and material density $\rho_{al} = 2645.19\,\text{kg/m}^3$. Similar details for mild steel pipes are: $L = 0.82$ m, $D_o = 0.032$ m, $D_i = 0.0195$ m and $\rho_{ms} = 7860\,\text{kg/m}^3$. For testing with water-filled conditions, one end of the pipe was closed by welding a cap. The other end was closed by a threaded stainless-steel end cap, which was connected by a pipe to a hand operated hydraulic pump. To facilitate supporting of the specimen two end supports were specially fabricated. These were fixed on a

Table 2
Measured rotational spring stiffness for aluminum pipes through deflection measurement

Case	Empty pipe				Water-filled pipe				Water-filled pipe				Water-filled pipe			
					Gauge pressure $p = 0$				Gauge pressure $p = 0.4905$ MPa				Gauge pressure $p = 0.981$ MPa			
	$\delta_{nc} \times 10^{-6}$ (m)	$\delta_c \times 10^{-6}$ (m)	K (MN/m)	$K_{average}$ (MN/m)	$\delta_{nc} \times 10^{-6}$ (m)	$\delta_c \times 10^{-6}$ (m)	K (MN/m)	$K_{average}$ (MN/m)	$\delta_{nc} \times 10^{-6}$ (m)	$\delta_c \times 10^{-6}$ (m)	K (MN/m)	$K_{average}$ (MN/m)	$\delta_{nc} \times 10^{-6}$ (m)	$\delta_c \times 10^{-6}$ (m)	K (MN/m)	$K_{average}$ (MN/m)
1	312.75	313.04	16.5950		315.651	315.94	16.8312		315.60	315.88	17.3691		315.48	315.75	17.9470	
2	311.25	311.55	15.9470	16.0558	313.75	314.04	16.7320	16.3000	313.75	314.06	15.5960	16.2521	313.80	314.10	16.0575	16.2520
3	305.75	306.05	15.6254		307.20	307.51	15.3370		307.25	307.55	15.7912		307.10	307.42	14.7513	
4	312.75	313.22	10.2394		315.65	316.12	10.3852		315.60	316.06	10.5725		315.48	315.95	10.3100	
5	311.25	311.74	9.7637	9.3161	313.75	314.24	9.9027	9.4950	313.75	314.24	9.8669	9.4450	313.80	314.30	9.6345	9.3151
6	305.75	306.34	7.9451		307.20	307.78	8.1972		307.25	307.85	7.8956		307.10	307.69	8.0007	
7	312.75	313.98	3.9126		315.65	316.94	3.7837		315.60	316.83	3.9539		315.48	316.77	3.7564	
8	311.25	312.55	3.6802	3.7057	313.75	315.05	3.7326	3.6970	313.75	315.08	3.6352	3.6823	313.80	315.11	3.6773	3.6020
9	305.75	307.08	3.5245		307.20	308.53	3.5747		307.25	308.62	3.4579		307.10	308.50	3.3717	
10	312.75	317.30	1.0577		315.65	320.20	1.0728		315.60	320.15	1.0689		315.48	320.00	1.0721	
11	311.25	315.80	1.0515	1.0435	313.75	318.35	1.0549	1.0538	313.75	318.36	1.0488	1.0383	313.80	318.39	1.0495	1.0493
12	305.75	310.34	1.0213		307.20	311.80	1.0336		307.25	312.00	0.9973		307.10	311.70	1.0262	

Table 3
Measured rotational spring stiffness for mild steel pipes through deflection measurement

Case	Empty pipe				Water-filled pipe				Water-filled pipe				Water-filled pipe			
					Gauge pressure $p = 0$				Gauge pressure $p = 0.4905$ MPa				Gauge pressure $p = 0.981$ MPa			
	$\delta_{nc} \times 10^{-6}$ (m)	$\delta_c \times 10^{-6}$ (m)	K (MN/m)	$K_{average}$ (MN/m)	$\delta_{nc} \times 10^{-6}$ (m)	$\delta_c \times 10^{-6}$ (m)	K (MN/m)	$K_{average}$ (MN/m)	$\delta_{nc} \times 10^{-6}$ (m)	$\delta_c \times 10^{-6}$ (m)	K (MN/m)	$K_{average}$ (MN/m)	$\delta_{nc} \times 10^{-6}$ (m)	$\delta_c \times 10^{-6}$ (m)	K (MN/m)	$K_{average}$ (MN/m)
1	75.30	75.42	23.2510	22.0165	76.25	76.37	23.5638	22.3128	76.00	76.13	21.7274	23.7220	76.35	76.47	23.5121	24.5120
2	62.20	62.31	20.782		63.37	63.48	21.0618		63.40	63.49	25.7163		63.25	63.34	25.6911	
3	75.30	75.52	12.6822	12.3570	76.25	76.47	12.853	12.8621	76.00	76.21	13.4503	13.1693	76.35	76.56	3.4355	13.5183
4	62.20	62.39	12.0317		63.37	63.55	12.8711		63.40	63.58	12.8582		63.25	63.42	13.6010	
5	130.85	131.45	8.4101	8.2975	132.25	132.83	8.8172	8.5561	132.00	132.58	8.8048	8.6183	132.40	132.95	9.2719	8.9227
6	121.80	122.37	8.1848		122.75	123.32	8.2950		122.00	122.56	8.4317		121.80	122.35	8.5734	
7	130.85	131.88	4.8991	4.8794	132.25	133.27	5.0137	4.9441	132.00	132.04	4.9104	4.8643	132.40	133.37	5.2572	5.0344
8	121.80	122.76	4.8597		122.75	123.72	4.8744		122.00	22.98	4.8181		121.80	122.78	4.8116	

Table 4
Predicted stiffness and crack location for aluminum pipes through frequency measurement ($L = 0.87$ m, $D_o = 0.033$ m, $D_i = 0.02$ m, $E_{empty\ pipe} = 60.3478$ GPa, $E_{water\text{-}filled\ pipe} = 61.6181$ GPa)

Actual data		Natural frequencies (Hz)			Predicted data		
β	a/t	ω_2	ω_3	ω_4	K (MN/m)	β	% error in β
Empty pipe							
No crack		382.50	835.0	1390.00			
		382.50[a]	860.63[a]	1530.00[a]			
0.207	0.19043	382.42	834.85	1389.90	16.387	0.205	−0.20
	0.25385	382.37	834.75	1389.85	9.900	0.202	−0.50
	0.38077	382.20	834.20	1389.45	3.613	0.189	−1.80
	0.63460	381.30	832.70	1389.10	1.050	0.225	−1.80
0.284	0.19043	382.42	834.95	1389.95	15.467	0.280	−0.40
	0.25385	382.38	834.92	1389.90	9.532	0.281	−0.30
	0.38077	382.20	834.85	1389.70	3.875	0.291	−0.70
	0.63460	381.40	834.40	1389.30	1.120	0.278	−0.60
0.397	0.25385	382.42	834.92	1389.50	8.833	0.375	−2.20
	0.38077	382.38	834.75	1388.65	3.350	0.405	−0.80
	0.63460	381.95	834.00	1385.70	0.960	0.395	−0.20
Water-filled pipe							
Gauge pressure $p = 0$							
No crack		350.00	775.00	1317.50			
		350.00[a]	787.50[a]	1400.00[a]			
0.207	0.19043	349.93	774.85	1317.45	16.000	0.215	0.80
	0.25385	349.88	774.77	1317.40	9.820	0.212	0.50
	0.38077	349.72	774.20	1317.00	3.493	0.188	−1.90
	0.63460	348.85	772.75	1316.65	1.002	0.215	0.80
0.284	0.19043	349.93	774.95	1317.45	15.767	0.277	−0.70
	0.25385	349.88	774.90	1317.40	8.867	0.276	−0.80
	0.38077	349.70	774.85	1317.20	3.702	0.287	0.30
	0.63460	348.85	774.50	1316.85	1.075	0.286	0.20
0.397	0.25385	349.95	774.90	1317.00	8.750	0.400	0.30
	0.38077	349.85	774.75	1316.20	3.350	0.391	−0.60
	0.63460	349.50	774.00	1313.20	0.965	0.393	−0.40

[a] Natural frequency of uncracked pipe calculated analytically.

vibration table at a required spacing by T-bolts. The setup is shown in Figs. 2–4. Pressure of fluid is directly noted from the pressure gauge of the hand pump. A total of 17 specimens (including two virgin specimens, one each for the two materials) were considered for the vibration test. Span length $L = 0.87$ m for aluminium and $L = 0.8$ m for mild steel pipes. The same specimens were used for static deflection measurement test with span length 0.7 and 0.74 m for aluminium and steel, respectively. Various dimensional combinations considered are shown in Table 1. The effect of overhang was neglected. Crack sizes in the ranges $a/t = 0.19-0.64$, where a is the edge crack size and t is the pipe wall thickness, were examined. The cracks were generated through wire-cut machining. The wire diameter was 0.15 mm.

Table 5
Predicted stiffness and crack location for aluminum pipes through frequency measurement ($L = 0.87$ m, $D_o = 0.033$ m, $D_i = 0.02$ m, $E_{p=0.4905\ \text{MPa}} = 62.4428$ GPa, $E_{p=0.981\ \text{MPa}} = 62.828$ GPa)

Actual data		Natural frequencies (Hz)			Predicted data		
β	a/t	ω_2	ω_3	ω_4	K (MN/m)	β	% error in β
Water-filled pipe							
Gauge pressure $p = 0.4905$ MPa							
No crack		352.500	777.50	1319.50			
		352.50[a]	792.92[a]	1409.50[a]			
0.207	0.19043	352.44	777.34	1319.44	17.083	0.202	−0.50
	0.25385	352.38	777.26	1319.41	9.875	0.201	−0.60
	0.38077	352.22	776.70	1319.00	3.547	0.188	−1.90
	0.63460	351.34	775.24	1318.68	1.040	0.214	0.70
0.284	0.19043	352.43	777.46	1319.42	15.683	0.288	0.40
	0.25385	352.40	777.41	1319.38	10.200	0.278	−0.60
	0.38077	352.22	777.37	1319.15	3.930	0.290	−0.60
	0.63460	351.37	777.00	1318.88	1.100	0.281	−0.30
0.397	0.25385	352.46	777.42	1319.00	8.567	0.410	1.30
	0.38077	352.36	777.26	1318.22	3.450	0.394	−0.30
	0.63460	352.10	776.55	1315.20	0.977	0.408	1.10
Water-filled pipe							
Gauge pressure $p = 0.981$ MPa							
No crack		353.75	779.25	1321.00			
		353.75[a]	795.53[a]	1414.01[a]			
0.207	0.19043	353.68	779.12	1320.95	17.625	0.217	1.00
	0.25385	353.62	779.05	1320.92	10.977	0.220	1.30
	0.38077	353.48	778.43	1320.50	3.568	0.188	−1.90
	0.63460	352.65	777.10	1320.15	1.092	0.214	0.70
0.284	0.19043	353.68	779.22	1320.93	17.020	0.290	0.60
	0.25385	353.65	779.18	1320.90	11.120	0.280	−0.40
	0.38077	353.45	779.10	1320.75	3.938	0.281	−0.30
	0.63460	352.65	778.80	1320.40	1.177	0.282	−0.20
0.397	0.25385	353.68	779.18	1320.50	9.013	0.382	−1.50
	0.38077	353.65	779.00	1319.75	3.267	0.415	1.80
	0.63460	353.30	778.30	1316.75	1.013	0.395	−0.20

[a] Natural frequency of uncracked pipe calculated analytically.

4.1. Deflection method

To facilitate determination of K through deflection measurements, a load was applied to the virgin specimen and the deflection was measured. Similar deflections were obtained by varying the load. A linear behavior was observed. A cracked specimen of the same geometry was then loaded at the same location and the load point deflection was measured. In this case too a linear behavior was observed. This procedure was repeated for all specimens for the two materials. The deflections were measured using a dial gauge with a least count of 0.001 mm. For each material four crack sizes were examined. In the case of aluminium, for each crack size, three positions were

Table 6
Predicted stiffness and crack location for mild steel pipes through frequency measurement ($L = 0.8$ m, $D_o = 0.032$ m, $D_i = 0.0195$ m, $E_{empty\ pipe} = 173.808$ GPa, $E_{water\text{-}filled\ pipe} = 178.328$ GPa)

Actual data		Natural frequencies (Hz)			Predicted data		
β	a/t	ω_2	ω_3	ω_4	K(MN/m)	β	% error in β
Empty pipe							
No crack		432.50	925.15	1602.50			
		432.50[a]	973.12[a]	1730.00[a]			
0.199	0.2032	432.33	924.80	1602.40	21.47	0.210	1.10
	0.3040	432.20	924.50	1602.00	12.51	0.205	0.60
0.403	0.4064	432.25	924.85	1600.80	8.21	0.384	−1.90
	0.5080	432.20	924.65	1599.50	4.79	0.390	−1.30
Water-filled pipe							
Gauge pressure $p = 0$							
No crack		422.50	905.00	1587.50			
		422.5	950.62[a]	1690.00[a]			
0.199	0.2032	422.30	904.65	1587.40	20.13	0.220	2.10
	0.3040	422.20	904.30	1587.00	12.21	0.196	−0.30
0.403	0.4064	422.25	904.70	1585.70	8.02	0.390	−1.30
	0.5080	422.15	904.50	1584.50	4.94	0.395	−0.80

[a] Natural frequency of uncracked pipe calculated analytically.

Table 7
Predicted stiffness and crack location for mild steel pipes through frequency measurement ($L = 0.8$ m, $D_o = 0.032$ m, $D_i = 0.0195$ m, $E_{p=0.4905\ \mathrm{MPa}} = 179.5433$ GPa, $E_{p=0.981\ \mathrm{MPa}} = 180.5503$ GPa)

Actual data		Natural frequencies (Hz)			Predicted data		
β	a/t	ω_2	ω_3	ω_4	K (MN/m)	β	% error in β
Water-filled pipe							
Gauge pressure $p = 0.4905$ MPa							
No crack		424.00	907.50	1590.00			
		424.00[a]	953.92[a]	1695.81[a]			
0.199	0.2032	423.78	906.18	1590.35	20.28	0.220	2.10
	0.3040	423.72	905.85	1590.10	13.00	0.196	−0.30
0.403	0.4064	423.78	906.20	1588.75	8.42	0.388	−1.50
	0.5080	423.70	905.90	1587.55	4.99	0.398	−0.50
Water-filled pipe							
Gauge pressure $p = 0.981$ MPa							
No crack		425.25	908.00	1593.00			
		425.25[a]	956.66[a]	1700.62[a]			
0.199	0.2032	425.06	907.68	1592.94	21.02	0.225	2.60
	0.3040	424.98	907.35	1592.55	13.22	0.192	−0.70
0.403	0.4064	425.10	907.75	1591.25	8.54	0.410	0.70
	0.5080	424.95	907.60	1590.20	5.50	0.392	−1.10

[a] Natural frequency of uncracked pipe calculated analytically.

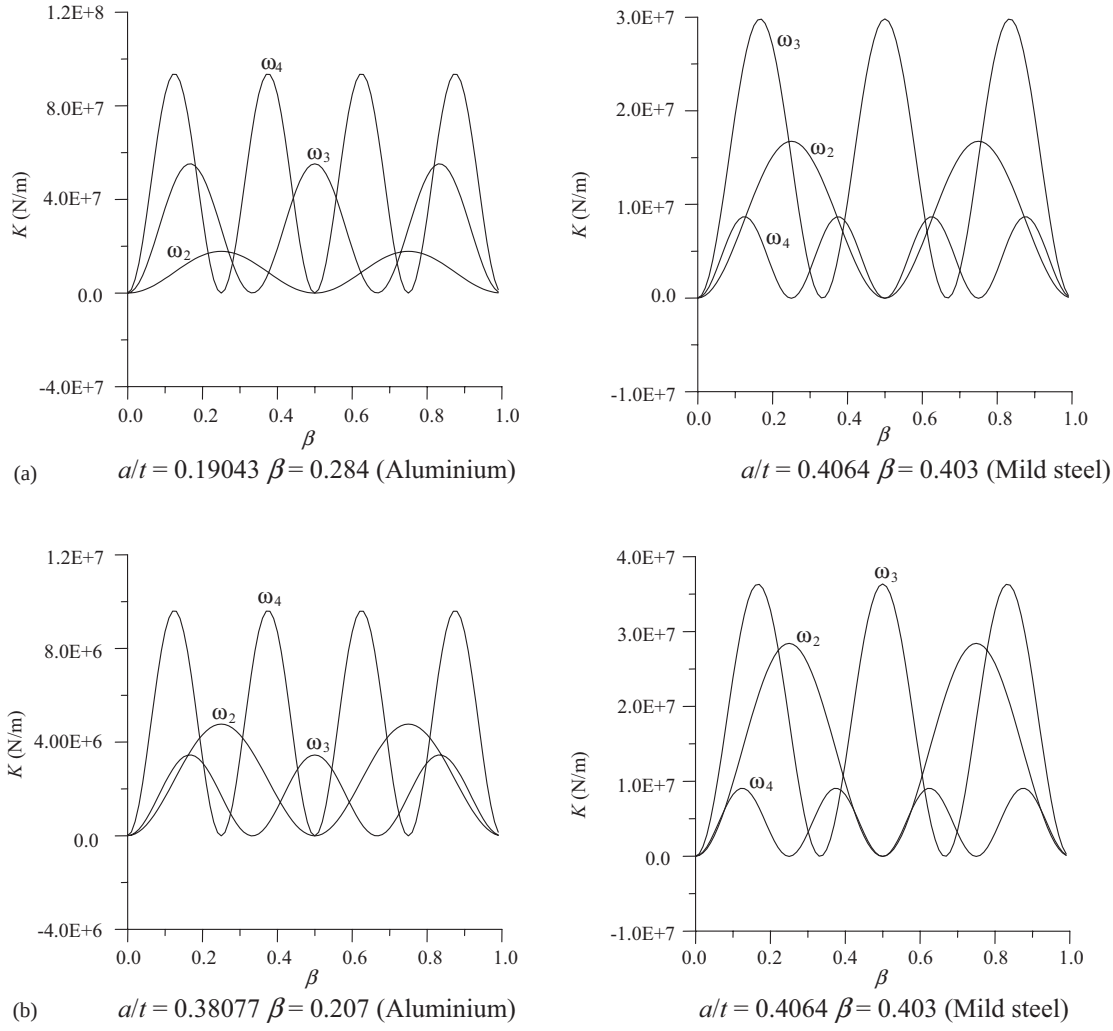

Fig. 5. Plots of stiffness K vs. crack location β for water-filled pipe: (a) no pressure, (b) gauge pressure = 0.981 MPa.

considered. In each case a load 147.15 N was applied in the transverse direction, i.e., along the crack line. In the case of steel, a similar combination was considered except that only two crack positions were taken instead of three. Experimental data for various dimensional combinations (Table 1) are shown in Tables 2 and 3.

4.2. Vibration method

To measure the natural frequencies an accelerometer (Type 4374, Bruel & Kjaer, Denmark) with a mass of 0.65 g was fixed on the top of the specimens using wax at a distance of 0.2 m from one of the ends. The output of the accelerometer was amplified by a charge amplifier (Type 5974, Bruel & Kjaer, Denmark) and was finally analyzed using a FFT analyzer (Type R9211A,

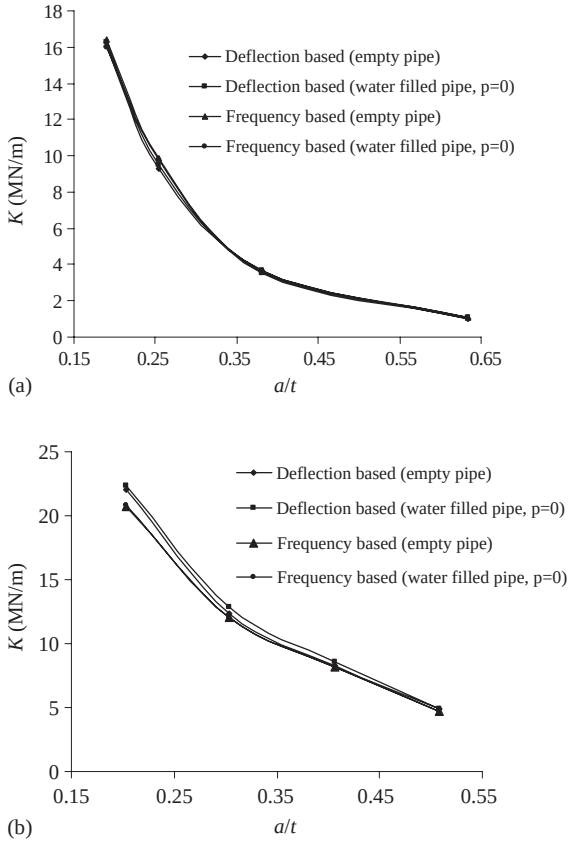

Fig. 6. Comparison of variation of stiffness K with crack size a/t for (a) aluminum and (b) mild steel pipes obtained by two methods for different internal conditions.

Advantest, Japan). The frequencies corresponding to the first few peaks are the natural frequencies of the pipe.

During testing a pipe was lightly tapped by a hammer in the transverse direction and the first few natural frequencies, first to fourth, were measured from the frequency responses. Frequencies for both cracked and the corresponding uncracked pipes were obtained. The experimental data for the second, third and fourth frequencies are shown in Tables 4–7. The first showed minimal difference between the uncracked and cracked pipes and it has not been included. The first two tables present results for aluminium; the last two show the same for mild steel. The experimental and analytical uncracked pipe frequencies are required for zero setting, while solving an inverse problem [8]. The uncracked pipe frequencies obtained analytically are also shown in these tables. To use appropriate data, Young's modulus of elasticity E was calculated through the measured second natural frequency of the uncracked empty pipe. The values obtained are 60.3478 and 173.808 GPa for aluminium and steel, respectively. These show a difference with the standard values by about 14%. The data for the water-filled pipes were also obtained in a similar manner. These are shown in Tables 4–7. As the water pressure increased, the modulus of elasticity showed a marginal increase.

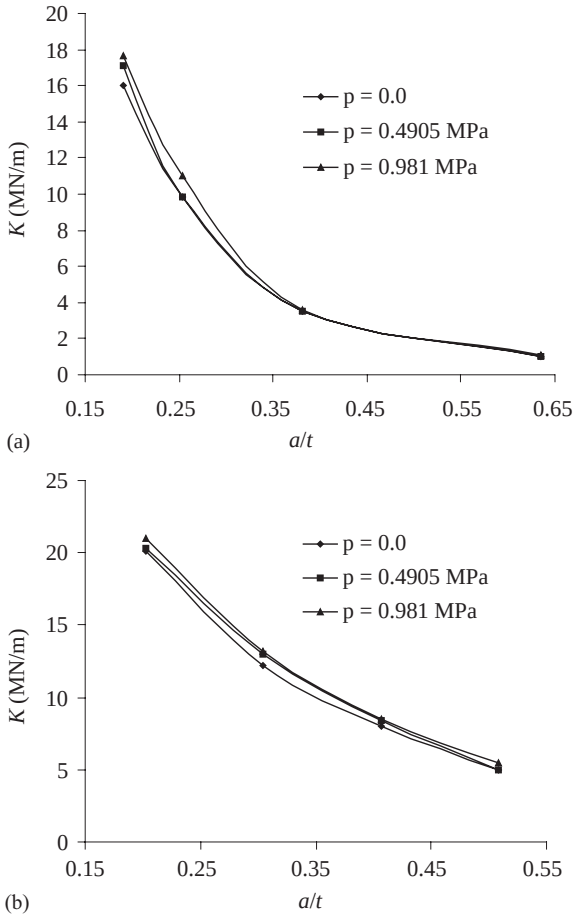

Fig. 7. Comparison of variation of stiffness K with crack size a/t for (a) aluminum and (b) mild steel for different fluid pressure obtained by frequency-based method.

5. Results on stiffness and crack prediction

The rotational spring stiffnesses calculated using Eqs. (11) and (12) for empty and water-filled conditions, respectively, are also shown in the tables. In the case of aluminium, for each crack size three crack positions are considered, and hence three stiffnesses are obtained. Since the rotational spring stiffness does not depend on crack positions the average of these three values is taken as the rotational spring stiffness. These are shown in Table 2. The similar results, but an average of two stiffnesses for mild steel, are shown in Table 3. Based on these observations it is found that the stiffness of pipe filled with water at no pressure differ from that of the empty pipe at the most by 1.92% and 10.065% for aluminium and mild steel, respectively. For the two cases of water under pressure (0.4905 and 0.981 MPa), the stiffnesses differ from that of the water-filled pipe at no pressure by at the most 1.471% and 2.57%, respectively, for aluminium, 6.316% and 10.26%, respectively, for mild steel.

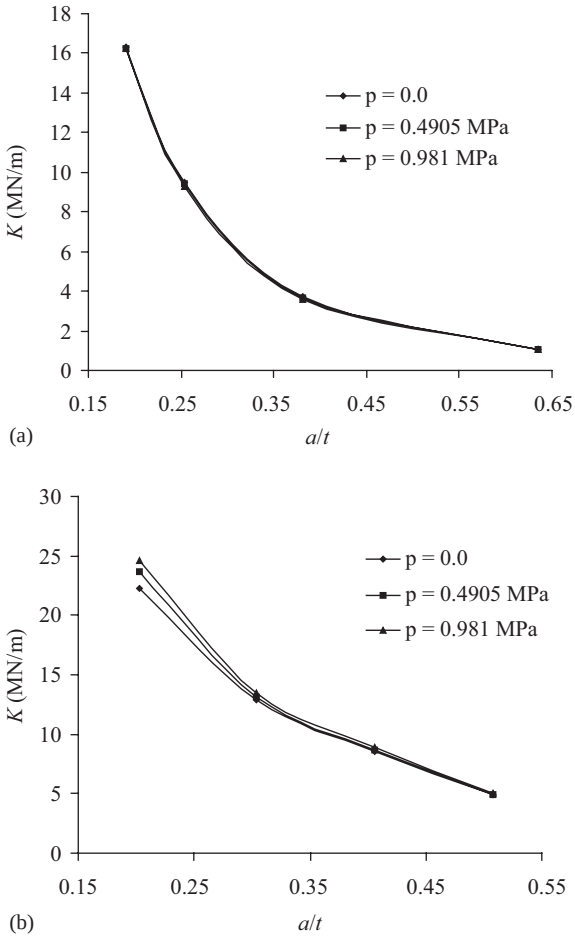

Fig. 8. Comparison of variation of stiffness K with crack size a/t for (a) aluminum and (b) mild steel for different fluid pressure obtained by deflection-based method.

To get the stiffness through the inverse analysis, for a particular crack size, variation of rotational spring stiffness with crack position along the beam length is obtained using Eq. (7) corresponding to each of the three frequencies. These three variations, K vs. crack location, are plotted. Typical plots are shown in Fig. 5. The intersection of the three curves gives the rotational spring stiffness. In case the curves do not intersect exactly at a point, the center of gravity of the three intersections is taken to obtain the stiffness [17]. The results are shown in Tables 4 and 5 for aluminium and Tables 6 and 7 for mild steel pipes. The stiffness in the case of pipe filled with water at no pressure differ with that of the empty pipe at the most by 4.571% and 6.241% for aluminium and mild steel, respectively. The similar difference in the case of water under pressure 0.4905 and 0.981 MPa is 6.77% and 11.78%, respectively, for aluminium and 6.47% and 10.88%, respectively, for steel. The stiffness obtained by the frequency method differs from that obtained through deflection techniques by 6.268% and 5.518% for empty and water-filled pipes of

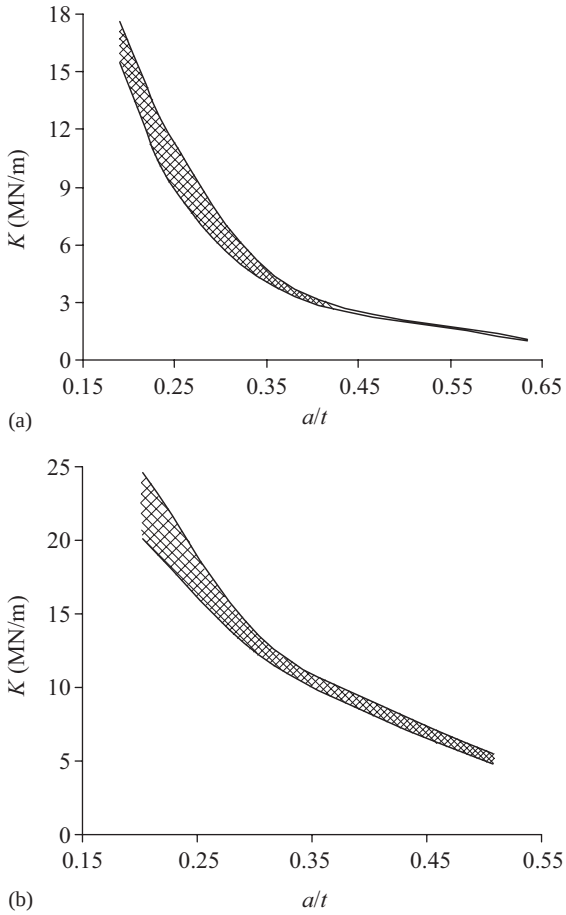

Fig. 9. Band of variation of stiffness K with crack size a/t for (a) aluminum and (b) mild steel.

aluminium, respectively. The similar differences for the mild steel pipes are 2.482% and 9.783%, respectively. The results by the two methods are therefore very close. The variations of rotational spring stiffness with crack size are shown in Figs. 6–8. These results are combined to show the band in variation in Fig. 9. Since a closed form relation between the rotational spring stiffness and crack size is not available, these plots can be very helpful in crack detection; crack size can be obtained given a spring stiffness.

Plots of variations of rotational spring stiffness K with crack location β (Fig. 5) helps to predict the crack location as well. The results so obtained are presented in Tables 4–7. The maximum errors in the prediction are less than 2.2% and 2.6% for aluminium and mild steel pipes, respectively. The vibration method can therefore be employed for prediction of crack location.

The crack size has been predicted using Fig. 9. These are shown in Table 8 for one crack position only ($\beta = 0.284$ for aluminium and $\beta = 0.199$ for mild steel). The error in size lies in the range -16.44% to 10.30% for aluminium and -5.83% to 12.04% for mild steel.

Table 8
Accuracy of prediction of crack size

Actual a/t	Predicted crack data				
	K(MN/m)	a/t		% error in a/t	
		Min	Max.	Min.	Max.
Aluminium empty pipe					
0.19043	15.467	0.191	0.207	0.30	8.00
0.25385	9.532	0.240	0.271	−5.77	6.33
0.38077	3.875	0.357	0.375	−6.66	−1.54
0.63460	1.120	0.563	0.624	−12.72	−1.70
Aluminium pipe with water at $p = 0$					
0.19043	15.767	0.186	0.204	−2.38	6.65
0.25385	8.867	0.252	0.283	−0.73	10.30
0.38077	3.702	0.364	0.382	−4.61	0.32
0.63460	1.075	0.568	0.615	−11.73	−3.20
Aluminium pipe with water at $p = 0.4905\ MPa$					
0.19043	15.683	0.188	0.205	−1.29	7.11
0.25385	10.200	0.233	0.264	−8.95	3.85
0.38077	3.930	0.358	0.374	−6.36	−1.81
0.63460	1.100	0.560	0.610	−13.32	−4.03
Aluminium pipe with water at $p = 0.981\ MPa$					
0.19043	17.020	0.181	0.195	−5.21	2.34
0.25385	11.120	0.223	0.253	−13.83	−0.34
0.38077	3.938	0.357	0.373	−6.66	−2.08
0.63460	1.177	0.545	0.581	−16.44	−9.23
Mild steel empty pipe					
0.2032	21.47	0.192	0.225	−5.83	9.69
0.3040	12.51	0.299	0.322	−1.67	5.59
Mild steel pipe with water at $p = 0$					
0.2032	20.13	0.203	0.231	−0.10	12.03
0.3040	12.21	0.302	0.328	−0.66	7.32
Mild steel pipe with water at $p = 0.4905\ MPa$					
0.2032	20.28	0.200	0.231	−1.60	12.04
0.3040	13.00	0.290	0.313	−4.83	2.88
Mild steel pipe with water at $p = 0.981\ MPa$					
0.2032	21.02	0.195	0.225	−4.21	9.69
0.3040	13.22	0.288	0.310	−5.56	1.94

6. Conclusions

The utility of representing a crack by a rotational spring in a straight component like an empty pipe for modelling its transverse free vibration for solving both the forward and inverse problems has been extended to include pipes filled with a fluid like water at varying (gauge) pressures. The rotational spring stiffness for pipes of two different materials and dimensions have been measured through the displacement- and vibration-based methods. There is a good agreement between the results obtained by the two methods. The relationships between the stiffness and crack size have been obtained. These will be useful for predicting crack sizes. The present effort to predict crack locations in the pipes show encouraging trend; the error is less than 2.6%. The error in crack size prediction lies in the range −16.44% to 12.04%.

References

[1] W.M. Ostachowicz, M. Krawczuk, Analysis of the effect of cracks on the natural frequencies of a cantilever beam, Journal of Sound and Vibration 150 (1991) 191–201.
[2] A.K. Pandey, M. Biswas, M.M. Samman, Damage detection from changes in curvature mode shapes, Journal of Sound and Vibration 145 (1991) 321–332.
[3] T.G. Chondros, A.D. Dimarogonas, Vibration of a cracked cantilever beam, Transactions of the American Society of Mechanical Engineers, Journal of Vibration and Acoustics 120 (1998) 742–746.
[4] A.D. Dimarogonas, Vibration of cracked structures: a state of the art review, Engineering Fracture Mechanics 55 (1996) 831–857.
[5] M.N. Cerri, F. Vestoroni, Detection of damage in beams subjected to diffused cracking, Journal of Sound and Vibration 234 (2000) 259–276.
[6] R.Y. Liang, F.K. Choy, J. Hu, Detection of cracks in beam structures using measurements of natural frequencies, Journal of the Franklin Institute 328 (1991) 505–518.
[7] X.F. Yang, A.S.J. Swamidas, R. Seshadri, Crack identification in vibrating beams using the energy method, Journal of Sound and Vibration 244 (2000) 339–357.
[8] B.P. Nandwana, S.K. Maiti, Detection of the location and size of a crack in stepped cantilever beams based on measurement of natural frequencies, Journal of Sound and Vibration 203 (1997) 435–446.
[9] B.P. Nandwana, S.K. Maiti, Modelling of vibration of beam in presence of inclined edge and internal crack for its possible detection based on frequency measurements, Engineering Fracture Mechanics 58 (1997) 93–205.
[10] T.D. Chaudhari, S.K. Maiti, Modelling of transverse vibration of beam of linearly variable depth with edge crack, Engineering Fracture Mechanics 63 (1999) 425–445.
[11] T.D. Chaudhari, S.K. Maiti, Experimental verification of a method of detection of crack in taper and segmented beams based on modeling of transverse vibration, International Journal of Fracture 102 (2000) 33–38.
[12] T.D. Chaudhari, S.K. Maiti, A study of vibration of geometrically segmented beams with and without crack, International Journal of Solids and Structures 37 (2000) 761–779.
[13] D.P. Patil, S.K. Maiti, Modelling of geometrically segmented beams to facilitate crack detection using frequency measurements, Proceedings of the 18th Canadian Congress of Applied Mechanics, Newfoundland, Canada, 2001, pp. 75–76.
[14] Y. Narkis, Identification of crack location in vibrating simply supported beam, Journal of Sound and Vibration 172 (1994) 549–558.
[15] A.P. Bovsunovsky, V.V. Matveev, Analytical approach to the determination of dynamic characteristics of a beam with a closing crack, Journal of Sound and Vibration 235 (2000) 415–435.
[16] T.D. Chaudhari, S.K. Maiti, Modelling of transverse vibration of circular and I-section beams with open edge crack to facilitate solving forward and inverse problems, Proceedings of the 18th Canadian Congress of Applied Mechanics, Newfoundland, Canada, 2001, pp. 77–78.

[17] B.P. Nandwana, On foundation for detection of crack based on measurement of natural frequencies, Ph.D. Thesis, Department of Mechanical Engineering, Indian Institute of Technology Bombay, 1997.
[18] S. Chinchalkar, Determination of crack location in beams using natural frequencies, Journal of Sound and Vibration 247 (2001) 417–429.
[19] A. Morassi, Identification of a crack in a rod based on changes in a pair of natural frequencies, Journal of Sound and Vibration 242 (2001) 577–596.
[20] M. Boltezar, B. Strancar, A. Kuhelj, Identification of transverse crack location in flexural vibrations of free–free beams, Journal of Sound and Vibration 211 (1998) 729–734.
[21] M.F. Yuen, A numerical study of the eigenparameters of a damaged cantilever, Journal of Sound and Vibration 103 (1985) 301–310.
[22] H. Tada, P.C. Paris, G.R. Irwin, The Stress Analysis of Cracks Handbook, 3rd Edition, ASME Press, New York, 2000.
[23] M.P. Paidousssis, G.X. Li, Pipes conveying fluid: a model dynamical problem, Journal of Fluids and Structures 7 (1993) 137–204.